Ain Shams Engineering Journal (2015) 6, 355–362

Ain Shams University

Ain Shams Engineering Journal

www.elsevier.com/locate/asej
www.sciencedirect.com

ENGINEERING PHYSICS AND MATHEMATICS

Flow of a Jeffrey fluid between torsionally oscillating disks

G. Bhaskar Reddy [a], S. Sreenadh [a], R. Hemadri Reddy [b,*], A. Kavitha [b]

[a] Department of Mathematics, Sri Venkateswara University, Tirupati 517502, India
[b] School of Advanced Sciences, VIT University, Vellore 632014, India

Received 30 June 2014; revised 2 September 2014; accepted 9 September 2014
Available online 7 October 2014

KEYWORDS

Jeffrey fluid;
Torsionary oscillating disks;
Frequency

Abstract In this paper, the flow of Jeffrey fluid between two torsionally oscillating disks is studied. This problem is solved in two cases. The first case is one disk oscillating and the other is at rest and the second case is two disks are oscillating with same frequency and speed but with phase difference of 180°. We found that the radial–axial flow has a mean steady component and a fluctuating component of frequency twice that of the oscillating disk. When the Jeffrey parameter λ tends to zero, the results coincide with the corresponding Newtonian case obtained by Rosenblat.

1. Introduction

The study of torsional vibrations of break disks is very important especially in applications where high power transmission and high speed are present. The model of flow between torsional oscillating disks may be observed in the turbine–coupling–generator rotor system and frictionless bearings. The torsional oscillation of a plate in Newtonian fluids has been discussed by Rosenblat [1]. He obtained the solution by expanding velocity components and the pressure in powers of the amplitude of oscillation of the plate and showed that the solution is highly convergent within the boundary layer. He has also discussed the case when the fluid is confined between two torsionally oscillating plates [1]. Similar problems in Reiner–Rivlin fluids were discussed by Srivastava [2,3]. In 1959, Rosenblat examined the flow between torsionally oscillating disks in the two cases: (i) one disk oscillating and the other at rest and (ii) both disks oscillating with the same frequency and speed, but with a phase difference of 180°. He developed and investigated the transverse and radial–axial flows for both small and large Reynold numbers. The theoretical analysis has been extended by Rajeswari [4] for Reiner–Rivlin fluids. She found that the radial–axial flow has a mean steady component and a fluctuating component of frequency twice that of the oscillating disk, a result similar to that for the Newtonian case obtained by Rosenblat. Bhatnagar and Rajeswari [4] and Srivastava have studied the same problem for a special case of the Rivlin–Ericksen second order fluid. Frater [5] has discussed only the first case of oldroyd fluid. Bhatnagar and Rajeswari have found that a reversal of the direction of the steady secondary flow is a characteristic feature of the Rivlin–Ericksen fluid and pointed out that it is always possible to find a value of the Reynolds number above which the flow is in reversed direction. The flow of an

* Corresponding author. Mobile: +91 9791452220.
E-mail address: rhreddy@vit.ac.in (R. Hemadri Reddy).
Peer review under responsibility of Ain Shams University.

Production and hosting by Elsevier

http://dx.doi.org/10.1016/j.asej.2014.09.004

Nomenclature

u	radial velocity component	υ	kinematic viscosity
v	transverse velocity component	R	Reynolds number
w	axial velocity component	n	frequency
p	pressure	Ω	angular speed
ρ	density	$\frac{\Omega}{n}$	amplitude
μ	dynamic viscosity		
λ	Jeffrey parameter		

incompressible visco-elastic Maxwell fluid between two parallel infinite disks executing small torsional oscillations in their own plane is discussed by Verma [6]. He found that with the increase of relaxation time parameter the elastic effects dominate in the region away from the oscillating disk and for small relaxation time, viscous effects permeate the entire flow.

Verma et al. [7] studied the flow induced in a viscous incompressible fluid from small torsional oscillations of an impermeable infinite disk bounded coaxially by another stationary naturally permeable infinite disk. He found that the steady radial velocity increases in magnitude with an increase of Reynolds number. Raghupathi Rao et al. [8] investigated the flow of a viscous fluid confined between two torsionally oscillating disks oscillating with the same frequency, but rotating with different, angular speeds about axes normal to the disks but not coincident. Sharma et al., studied the flow of an incompressible second-order fluid due to torsional oscillations of two infinite disks. They found that the effect of second order forces increases the amplitude of the oscillation of the axial velocity. The unsteady MHD flow of an incompressible viscous electrically conducting fluid contained between two torsionally oscillating eccentric disks has been investigated by Ragupathi Rao. Torsional oscillation of an infinite disk in a viscous liquid bounded by a porous medium fully saturated with the liquid was discussed by Srivastava. He found that the depth of penetration of the flow in the porous medium is proportional to the square root of the permeability of the medium.

Srivastava et al. discussed the flow due to torsional oscillations of infinite disks at a small distance from the unbounded porous medium when the entire space between the disks and the porous medium is filled with a second grade fluid. The problem of the flow of an incompressible non-Newtonian second order fluid between two enclosed torsionally oscillating disks has been discussed by Singh et al.. The effects of transducer compliance on transient stress measurements in torsional flow of a viscoelastic fluid are investigated by Dutcher et al. [9]. Pawan kumar Sharma et al. [10] investigated the unsteady laminar flow of an incompressible viscous electrically conducting fluid in a porous medium fully saturated with the liquid and bounded by torsionally oscillating disk in the presence of a transverse magnetic field.

Nadeem et al. [11] studied the effect of Jeffrey fluid with variable viscosity in the form of a well known Reynolds model of viscosity in an asymmetric channel. Akbar et al. [12] discussed a non-Newtonian fluid model for a blood flow through a tapered artery with a stenosis by assuming blood as Jeffrey fluid. Nadeem et al. [13] discussed the closed form analytical and numerical solutions of the peristaltic flow of a Jeffrey fluid in an inclined tube with different viscosities and with different wave shapes. Non-Newtonian fluid model for blood flow through a tapered artery with a stenosis and variable viscosity by modeling blood as Jeffrey fluid has been studied by Akbar et al. [14]. The effect of temperature-dependent viscosity on the Peristaltic flow of Jeffrey fluid through the gap between two co-axial horizontal tubes was analyzed by Akbar et al. [15]. Akbar et al. [16] studied a non-Newtonian fluid model for blood flow through a tapered artery with a stenosis by assuming blood as Jeffrey fluid. Hayat et al. [17] examined the flow of an incompressible Jeffrey fluid over a stretching surface. Hayat et al. [18] described the mixed convection stagnation point flow and heat transfer of a Jeffrey fluid toward a stretching surface. The boundary layer stretched flow of a Jeffrey fluid subject to the convective boundary conditions was investigated by Hayat et al. [19].

In this chapter, the flow of Jeffrey fluid between two torsionally oscillating disks is studied. This problem is solved in two cases. The first case is one disk oscillating and the other is at rest and the second case is two disks are oscillating with same frequency and speed but with phase difference of 180°. We found that the radial–axial flow has a mean steady component and a fluctuating component of frequency twice that of the oscillating disk. When the Jeffrey parameter λ tends to zero, the results coincide with the corresponding Newtonian case obtained by Rosenblat.

2. Mathematical formulation

We consider a body of a Jeffrey fluid bounded by two Infinite parallel plane disks which are represented by the plane $z = 0$ and $z = d$ in a cylindrical polar co-ordinate system. The disks perform torsional oscillations about the axis $r = 0$. If u, v and w be respectively the radial, transverse and axial velocity components, p be the pressure, ρ be the density, μ is the dynamic viscosity, λ is the ratio of relaxation to retardation time and v is the kinematic viscosity.

The constitutive equations for Jeffrey fluid (Vajravelu et al., [20]) are

$$T = -PI + S$$

$$S = \frac{\mu}{1+\lambda_1}[\dot{\gamma} + \lambda_2 \ddot{\gamma}]$$

where P is pressure, S is extra stress tensor, T is the stress, I is identity tensor, μ is dynamic viscosity, λ_1 is the ratio of relaxation time and retardation times, λ_2 is the retardation time, γ is rate of strain tensor and the dots over the quantities denote differentiation. The quantities $\dot{\gamma}$ and $\ddot{\gamma}$ are defined by

$$\dot{\gamma} = \nabla\bar{q} + (\nabla\bar{q})^T$$

$$\ddot{\gamma} = \frac{d}{dt}\dot{\gamma} = \frac{\partial}{\partial t}\dot{\gamma} + (\bar{q}\cdot\nabla)\dot{\gamma}$$

where $\bar{q}$ the fluid velocity is vector and $\frac{d}{dt}$ is the material derivative. In the present investigation we assume that $\lambda_1 = \lambda$ and $\lambda_2 = 0$.

The equation of motion of a Jeffrey fluid in cylindrical polar coordinate system is

$$\frac{\partial u}{\partial t} + u\frac{\partial u}{\partial r} + w\frac{\partial u}{\partial z} - \frac{v^2}{r} = -\frac{1}{\rho}\frac{\partial p}{\partial r} + \frac{\nu}{1+\lambda}\left[\frac{\partial^2 u}{\partial r^2} + \frac{1}{r}\frac{\partial u}{\partial r} - \frac{u}{r^2} + \frac{\partial^2 u}{\partial z^2}\right] \quad (1)$$

$$\frac{\partial v}{\partial t} + u\frac{\partial v}{\partial r} + w\frac{\partial v}{\partial z} + \frac{uv}{r} = \frac{\nu}{1+\lambda}\left[\frac{\partial^2 v}{\partial r^2} + \frac{1}{r}\frac{\partial v}{\partial r} - \frac{v}{r^2} + \frac{\partial^2 v}{\partial z^2}\right] \quad (2)$$

$$\frac{\partial w}{\partial t} + u\frac{\partial w}{\partial r} + w\frac{\partial w}{\partial z} = -\frac{1}{\rho}\frac{\partial p}{\partial z} + \frac{\nu}{1+\lambda}\left[\frac{\partial^2 w}{\partial r^2} + \frac{1}{r}\frac{\partial w}{\partial r} + \frac{\partial^2 w}{\partial z^2}\right] \quad (3)$$

while the equation of continuity is

$$\frac{1}{r}\frac{\partial}{\partial r}(ru) + \frac{\partial w}{\partial z} = 0 \quad (4)$$

3. Solution of the problem

3.1. Case (1): One disk oscillating

We consider the disk at $z = 0$ to perform torsional oscillations of frequency 'n' and angular speed Ω, while the disk at $z = d$ remains at rest.

The boundary conditions for the problem are

$$\left.\begin{array}{lll} u = w = 0, & v = r\Omega e^{\mathrm{int}} & on\ z = 0 \\ u = v = w = 0 & & on\ z = d \end{array}\right\} \quad (5)$$

Eqs. (1)–(5) can be satisfied by writing

$$\left.\begin{array}{ll} v = r\Omega e^{i\tau} g(y), & u = \frac{r\Omega^2}{n}\frac{\partial F}{\partial y}(y,\tau) \\ w = -2d\frac{\Omega^2}{n}F(y,\tau), & y = \frac{z}{d},\quad \tau = nt \\ \frac{p}{\rho} = \Omega^2 d^2 p(y,\tau) + \frac{1}{2}\Omega^2 r^2 k(\tau) & \end{array}\right\} \quad (6)$$

On substitution from (6), Eqs. (1) and (2) become

$$\frac{\partial^2 F}{\partial y\partial\tau} + \left(\frac{\Omega}{n}\right)^2\left[\left(\frac{\partial F}{\partial y}\right)^2 - 2F\frac{\partial^2 F}{\partial y^2}\right] - \left(ge^{i\tau}\right)^2 = -k(\tau) + \frac{1}{R(1+\lambda)}\frac{\partial^3 F}{\partial y^3} \quad (7)$$

$$\text{and } ig + 2\left(\frac{\Omega}{n}\right)^2\left[g\frac{\partial F}{\partial y} - F\frac{dg}{dy}\right] = \frac{1}{R(1+\lambda)}\frac{d^2 g}{dy^2} \quad (8)$$

$$\text{where } R = \frac{nd^2}{\nu} \text{ is the Reynolds number of the flow.} \quad (9)$$

The boundary conditions (5) become

$$\left.\begin{array}{ll} F = \frac{\partial F}{\partial y} = 0, & g = 1 \quad on\ y = 0 \\ F = \frac{\partial F}{\partial y} = g = 0 & on\ y = 1 \end{array}\right\} \quad (10)$$

Eq. (3) reduces to

$$2\frac{\partial F}{\partial\tau} - 4\left(\frac{\Omega}{n}\right)^2 F\frac{\partial F}{\partial y} = \frac{\partial p}{\partial y} + \frac{2}{R(1+\lambda)}\frac{\partial^2 F}{\partial y^2} \quad (11)$$

and serves merely to determine the axial pressure gradient.

3.1.1. Transverse component

On the assumption that the amplitude of the oscillations namely $\frac{\Omega}{n}$ is small, retaining only the first order terms in $\frac{\Omega}{n}$, we have for the transverse velocity component

$$\left.\begin{array}{l} \frac{d^2 g}{dy^2} - iR(1+\lambda)g(y) = 0 \\ with\ g(0) = 1\ and\ g(1) = 0 \end{array}\right\} \quad (12)$$

The solution of (12) is

$$g(y) = \frac{\sinh\left[\sqrt{iR(1+\lambda)}(1-y)\right]}{\sinh\sqrt{iR(1+\lambda)}} \quad (13)$$

Eq. (13) leads to, in real notation,

$$\frac{v}{r\Omega} = \frac{\left[\cos\sqrt{\tfrac{1}{2}R(1+\lambda)}y\cosh\sqrt{\tfrac{1}{2}R(1+\lambda)}(2-y) - \cos\sqrt{\tfrac{1}{2}R(1+\lambda)}(2-y)\cosh\sqrt{\tfrac{1}{2}R(1+\lambda)}y\right]\cos nt}{\cosh\sqrt{2R(1+\lambda)} - \cos\sqrt{2R(1+\lambda)}} + \frac{\left[\sin\sqrt{\tfrac{1}{2}R(1+\lambda)}y\sinh\sqrt{\tfrac{1}{2}R(1+\lambda)}(2-y) - \sin\sqrt{\tfrac{1}{2}R(1+\lambda)}(2-y)\sinh\sqrt{\tfrac{1}{2}R(1+\lambda)}y\right]\sin nt}{\cosh\sqrt{2R(1+\lambda)} - \cos\sqrt{2R(1+\lambda)}} \quad (14)$$

Expanding this for small values of the Reynolds number, we have

$$\frac{v}{r\Omega} = (1-y)\left\{\left[1 - \frac{R^2(1+\lambda)^2}{360}y\left(3y^3 - 12y^2 + 8y + 8\right)\right]\cos nt + \frac{R}{6}(1+\lambda)y(2-y)\sin nt\right\} + 0(R^3) \quad (15)$$

With amplitude approximate

$$\frac{|v|}{r\Omega} = (1-y)\left[1 - \frac{R^2(1+\lambda)^2}{180}y(2-y)(2-2y+y^2)\right] \quad (16)$$

and phase angle is

Expanding this for small values of the Reynolds number

$$Tan^{-1}\left[\frac{\sin\sqrt{\frac{1}{2}R(1+\lambda)}y\sinh\sqrt{\frac{1}{2}R(1+\lambda)}(2-y)-\sin\sqrt{\frac{1}{2}R(1+\lambda)}(2-y)\sinh\sqrt{\frac{R}{2}(1+\lambda)}y}{\cos\sqrt{\frac{R}{2}(1+\lambda)}y\cosh\sqrt{\frac{R}{2}(1+\lambda)}(2-y)-\cos\sqrt{\frac{R}{2}(1+\lambda)}(2-y)\cosh\sqrt{\frac{R}{2}(1+\lambda)}y}\right] \tag{17}$$

$$Tan^{-1}\left[\frac{1}{6}R(1+\lambda)y(2-y)\right] \tag{18}$$

From the Eq. (15), the skin friction for small Reynolds number R on the disk $z = 0$ is

$$\frac{\mu}{1+\lambda}\left(\frac{\partial v}{\partial z}\right)_{z=0}\cong\frac{-\mu r\Omega}{d(1+\lambda)}\left[\left(1+\frac{R^2(1+\lambda)^2}{45}\right)\cos nt-\frac{R(1+\lambda)}{3}\sin nt\right] \tag{19}$$

and on the disk $z = d$ is

$$\frac{\mu}{1+\lambda}\left(\frac{\partial v}{\partial z}\right)_{z=d}=-\frac{\mu r\Omega}{d(1+\lambda)}\left[\left(1-\frac{7R^2(1+\lambda)^2}{360}\right)\cos nt+\frac{R(1+\lambda)}{6}\sin nt\right] \tag{20}$$

where $R\to 0$, the shearing forces are equal on the two disks. As R increases, the shear stress on the rotating disk increases in magnitude, while that on the stationary disk it decreases.

3.1.2. Steady radial–axial component

Neglecting the terms of order $\left(\frac{\Omega}{n}\right)^2$, we have from (7) for the radial–axial component of velocity.

$$\frac{\partial^2 F}{\partial y\partial\tau}-\left(ge^{i\tau}\right)^2=-k(\tau)+\frac{1}{R(1+\lambda)}\frac{\partial^3 F}{\partial y^3} \tag{21}$$

From (13) we obtain

$$\left(ge^{i\tau}\right)^2=\frac{1}{2}\left[\frac{\cosh s(1-y)-\cos s(1-y)}{\cosh s-\cos s}\right]+\frac{1}{2}\left[\frac{\cosh(1+i)s(1-y)-1}{\cosh(1+i)s-1}\right]e^{2i\tau} \tag{22}$$

where $s=\sqrt{2R(1+\lambda)}$.

This suggests that there are solutions of the form

$$F(y,\tau)=f(y)+h(y)e^{2i\tau} \tag{23}$$

$$k(\tau)=k_0+k_1e^{2i\tau} \tag{24}$$

and substitution of (22)–(24) into (21) yield

$$\frac{2}{s^2}\frac{d^3f}{dy^3}=k_0-\frac{1}{2}\left[\frac{\cosh s(1-y)-\cos s(1-y)}{\cosh s-\cos s}\right] \tag{25}$$

$$\frac{2}{s^2}\frac{d^3h}{dy^3}-2i\frac{dh}{dy}=k_1-\frac{1}{2}\left[\frac{\cosh(1+i)s(1-y)-1}{\cosh(1+i)s-1}\right] \tag{26}$$

The boundary conditions are

$$\left.\begin{aligned} f=f'=0 \quad & on\ y=0\ and\ y=1\\ h=h'=0 \quad & on\ y=0\ and\ y=1\end{aligned}\right\} \tag{27}$$

The solution of (25) for the mean steady component under the boundary conditions (27) is found to be

$$\begin{aligned}f(y)=\frac{1}{\cosh s-\cos s}\Big\{&\frac{1}{4s}(\sinh s(1-y)+\sin s(1-y))\\&-\frac{1}{4s}(\sinh s+\sin s)(1-3y^2+2y^3)\\&+\frac{1}{4}(\cosh s+\cos s)y(1-2y+y^2)-\frac{1}{2}y^2(1-y)\Big\}\end{aligned} \tag{28}$$

$$\begin{aligned}f'(y)=\frac{1}{\cosh s-\cos s}\Big\{&-\frac{1}{4}(\cos s(1-y)+\cos s(1-y))\\&+\frac{3}{2s}(\sinh s+\sin s)(1-y)y\\&+\frac{1}{4}(\cosh s+\cos s)(1-4y+3y^2)-\frac{1}{2}y(2-3y)\Big\}\end{aligned} \tag{29}$$

with $k_0=\frac{3}{s^3}\left[\frac{2s+s(\cosh s+\cos s)-2(\sinh s+\sin s)}{\cosh s-\cos s}\right]$

Here $s=\sqrt{2R(1+\lambda)}$

The results with $\lambda = 0$ corresponding to the Newtonian case are in agreement with those of Rosenblat.

3.1.3. Fluctuating radial–axial flow

The solution of (26) for the fluctuating radial–axial flow under the boundary conditions (27) is found to be

$$\begin{aligned}4i\ &[\cosh\alpha s-1]\alpha s\beta[2-2\cosh\beta s+\beta s\sinh\beta s]h(y)\\&=\cosh\beta sy[\alpha\sinh\beta s(\cosh\alpha s-1)+\alpha\beta s(1-\cosh\alpha s\cosh\beta s)\\&\quad+\beta\sinh\alpha s(\cosh\beta s-1)]\\&\quad+\sinh\beta y[\alpha(1-\cosh s\beta)(\cosh s\alpha-1)\\&\quad+\beta\sinh s\beta(s\alpha\cosh s\alpha-\sinh s\alpha)]\\&\quad+\alpha\sinh s\beta(1-\cosh s\alpha)+s\alpha\beta(\cosh s\alpha\cosh s\beta-1)\\&\quad-\beta\sinh s\alpha(1-\cosh s\beta+s\beta\sinh s\beta)\\&\quad+ys\beta[\beta\sinh s\alpha\sinh s\beta+\alpha(1-\cosh s\beta)(1+\cosh s\alpha)]\\&\quad+\beta\sinh s\alpha(1-y)[2-2\cosh s\beta+s\beta\sinh s\beta]\end{aligned} \tag{30}$$

where $\alpha=1+i$ *and* $\beta=\frac{1}{\sqrt{2}}(1+i)$

3.2. Case (II): Two disks are oscillating

We now consider the case when both the disks are oscillating with the same frequency and angular speed but in opposite directions.

The boundary conditions in the present case of the problem are

$$u = w = 0, \quad v = r\Omega e^{\text{int}} \quad on\ z = 0$$
$$u = w = 0, \quad v = -r\Omega e^{\text{int}} \quad on\ z = d$$

3.2.1. Transverse component

The Eqs. (1)–(4) can again be transformed by the choice of the velocity field (6) in a similar way and for the transverse flow, we have

$$\frac{d^2g}{dy^2} - iR(1+\lambda)g = 0 \tag{31}$$

The boundary conditions are

$$g(0) = 1,\ g(1) = -1$$

The solution now is

$$g(y) = \frac{\sinh\sqrt{iR(1+\lambda)}y_1 - \sinh\sqrt{ir(1+\lambda)}y}{\sinh\sqrt{iR(1+\lambda)}} \tag{32}$$

The real part of (32) is

$$\begin{aligned}
&\Big[\cos\sqrt{\tfrac{R}{2}(1+\lambda)}y\cosh\sqrt{\tfrac{R}{2}(1+\lambda)}(2-y) - \cos\sqrt{\tfrac{R}{2}(1+\lambda)}(2-y)\cosh\sqrt{\tfrac{R}{2}(1+\lambda)}y \\
&- \cos\sqrt{\tfrac{R}{2}(1+\lambda)}(y-1)\cosh\sqrt{\tfrac{R}{2}(1+\lambda)}(1+y) + \cos\sqrt{\tfrac{R}{2}(1+\lambda)}(y+1)\cosh\sqrt{\tfrac{R}{2}(1+\lambda)}(y-1)\Big]\cos nt \\
&+\Big[-\sin\sqrt{\tfrac{R}{2}(1+\lambda)}y\sinh\sqrt{\tfrac{R}{2}(1+\lambda)}(2-y) + \sin\sqrt{\tfrac{R}{2}(1+\lambda)}(y+1)\sin\sqrt{\tfrac{R}{2}(1+\lambda)}y \\
&-\sin\sqrt{\tfrac{R}{2}(1+\lambda)}(y-1)\sinh\sqrt{\tfrac{R}{2}(1+\lambda)}(y+1) + \sin\sqrt{\tfrac{R}{2}(1+\lambda)}(y+1)\sinh\sqrt{\tfrac{R}{2}(1+\lambda)}(y-1)\Big]\sin nt \\
\frac{v}{r\Omega} = &\frac{}{\cosh\sqrt{2R(1+\lambda)} - \cos\sqrt{2R(1+\lambda)}}
\end{aligned} \tag{33}$$

Expanding this for small values of the Reynolds number, we have

$$\frac{v}{r\Omega} = (1-2y)\left\{\left[1 - \frac{R^2(1+\lambda)^2}{360}y(1-y)(1+3y-3y^2)\right]\cos nt + \frac{R}{6}y(1-y)\sin nt\right\} + 0(R^3) \tag{34}$$

Hence the amplitude is given by

$$\frac{|v|}{r\Omega} = (1-2y)\left[1 - \frac{R^2(1+\lambda)^2}{360}y(1-y)(1-2y+2y^2)\right] \tag{35}$$

and phase angle is

$$Tan^{-1}\left\{\frac{\begin{array}{c}\Big[-\sin\sqrt{\frac{R}{2}(1+\lambda)}y\sinh\sqrt{\frac{R}{2}(1+\lambda)}(2-y) + \sin\sqrt{\frac{R}{2}(1+\lambda)}(y+1)\sin\sqrt{\frac{R}{2}(1+\lambda)}y \\ -\sin\sqrt{\frac{R}{2}(1+\lambda)}(y-1)\sinh\sqrt{\frac{R}{2}(1+\lambda)}(y+1) + \sin\sqrt{\frac{R}{2}(1+\lambda)}(y+1)\sinh\sqrt{\frac{R}{2}(1+\lambda)}(y-1)\Big]\end{array}}{\begin{array}{c}\Big[\cos\sqrt{\frac{R}{2}(1+\lambda)}y\cosh\sqrt{\frac{R}{2}(1+\lambda)}(2-y) - \cos\sqrt{\frac{R}{2}(1+\lambda)}(2-y)\cosh\sqrt{\frac{R}{2}(1+\lambda)}y \\ -\cos\sqrt{\frac{R}{2}(1+\lambda)}(y-1)\cosh\sqrt{\frac{R}{2}(1+\lambda)}(y+1) + \cos\sqrt{\frac{R}{2}(1+\lambda)}(y+1)\cosh\sqrt{\frac{R}{2}(1+\lambda)}(y-1)\Big]\end{array}}\right\} \tag{36}$$

Expanding this for small values of Reynolds number, we get

$$Tan^{-1}\frac{1}{6}R(1+\lambda)y(1-y) \tag{37}$$

The skin friction is given by

$$\begin{aligned}
&\tfrac{\mu}{1+\lambda}\left(\tfrac{\partial v}{\partial z}\right)_{z=0} = \tfrac{\mu}{1+\lambda}\left(\tfrac{\partial v}{\partial z}\right)_{z=d} \\
&= \tfrac{-2\mu r\Omega}{d(1+\lambda)}\left[\left(1 + \tfrac{R^2(1+\lambda)^2}{720}\right)\cos nt - \tfrac{R(1+\lambda)}{12}\sin nt\right]
\end{aligned} \tag{38}$$

For any value of R, the shearing forces are equal on the two disks. When R increases, the shear stress on the two disks in magnitude also increases.

3.2.2. Steady radial–axial component

Neglecting the terms of order $\left(\frac{\Omega}{n}\right)^2$, we have from (7) for the radial–axial component of velocity

$$\frac{\partial^2 F}{\partial y\partial\tau} - \left(ge^{i\tau}\right)^2 = -k(\tau) + \frac{1}{R(1+\lambda)}\frac{\partial^3 F}{\partial y^3} \tag{39}$$

From (32) we have

$$\begin{aligned}
[g(y)]^2 e^{2i\tau} = &\frac{\cosh\frac{s}{2} + \cos\frac{s}{2}}{\cosh s - \cos s}\left[\cosh\frac{s}{2}(1-2y) - \cos\frac{s}{2}(1-2y)\right] \\
&+ \frac{\cosh\frac{s}{2}(1+i) - 1}{\cosh s(1+i) - 1}\left[\cosh\frac{s}{2}(1+i)(1-2y) - 1\right]e^{i2\tau}
\end{aligned} \tag{40}$$

where $s = \sqrt{2R(1+\lambda)}$

Substitution of (23), (24) and (40) into (39) yields

$$\frac{2}{s^2}\frac{d^3 f}{dy^3} = k_0 - \frac{\cosh\frac{s}{2} + \cos\frac{s}{2}}{\cosh s - \cos s}\left[\cosh\frac{s}{2}(1-2y) - \cos\frac{s}{2}(1-2y)\right] \tag{41}$$

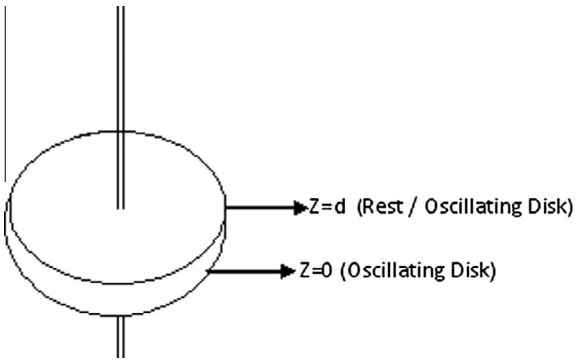

Figure 1 Physical model.

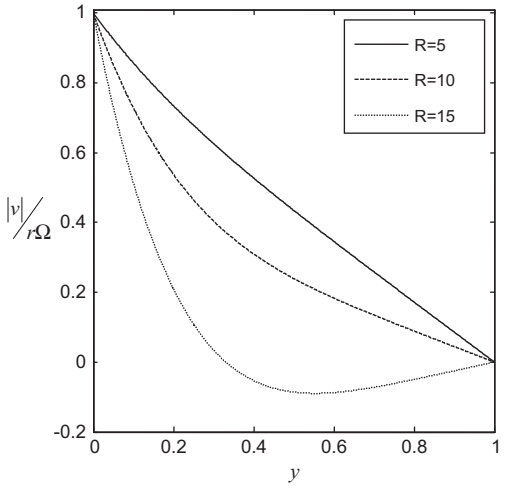

Figure 2 Variation of amplitude of transverse velocity $\frac{|v|}{r\Omega}$ with Reynolds number R for fixed value of $\lambda = 1$.

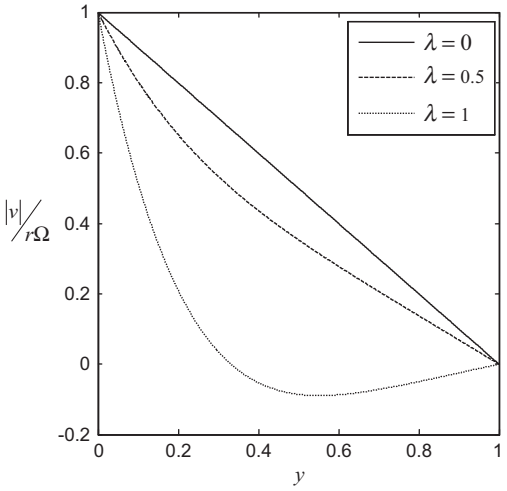

Figure 3 Variation of amplitude of transverse velocity $\frac{|v|}{r\Omega}$ with Jeffrey parameter λ for fixed value of $R = 20$.

$$\frac{2}{s^2}\frac{d^3h}{dy^3} - 2i\frac{dh}{dy} = k_1 - \frac{\cosh\frac{s}{2}(1+i)-1}{\cosh s(1+i)-1}\left[\cosh\frac{s}{2}(1+i)(1-2y)-1\right] \tag{42}$$

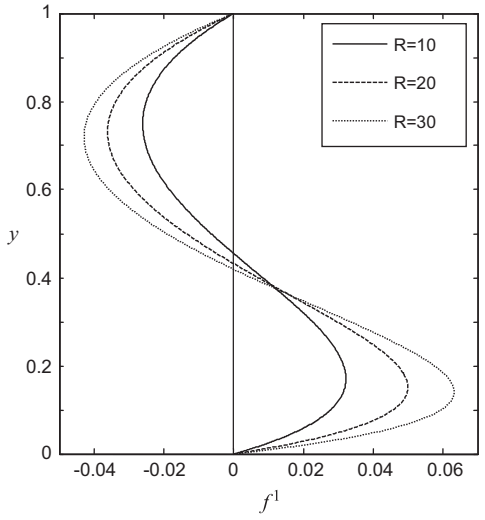

Figure 4 Variation of steady radial velocity f^1 with Reynolds number R for fixed value of $\lambda = 1$.

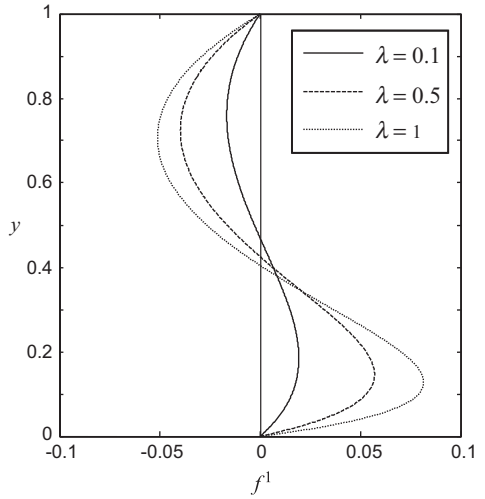

Figure 5 Variation of steady radial velocity f^1 with Jeffrey parameter λ for fixed value of $R = 20$.

The solution of (41) for the mean steady component under the boundary condition (27) is found to be

$$\begin{aligned} f(y) = {} & \frac{1}{2}\frac{\cosh\frac{s}{2}+\cos\frac{s}{2}}{\cosh s-\cos s}\left\{(2y^3-3y^2)\left(\cosh\frac{s}{2}-\frac{2}{s}\sinh\frac{s}{2}\right)+\frac{1}{s}\sinh\frac{s}{2}(1-2y)\right. \\ & +y\cosh\frac{s}{2}+(2y^3-3y^2)\left(\cos\frac{s}{2}-\frac{2}{s}\sin\frac{s}{2}\right) \\ & \left.+\frac{1}{s}\sin\frac{s}{2}(1-2y)+y\cos\frac{s}{2}-\frac{1}{s}\sin\frac{s}{2}\right\} \end{aligned} \tag{43}$$

$$\begin{aligned} f^1 = {} & \frac{1}{2}\left[\frac{\cosh\frac{s}{2}+\cos\frac{s}{2}}{\cosh s-\cos}\right]\left\{6(y^2-y)\left(\cosh\frac{s}{2}-\frac{2}{s}\sinh\frac{s}{2}\right)\right. \\ & +\cosh\frac{s}{2}-\cosh\frac{s}{2}(1-2y)+6(y^2-y)\left(\cos\frac{s}{2}-\frac{2}{s}\sin\frac{s}{2}\right) \\ & \left.+\cos\frac{s}{2}-\cos\frac{s}{2}(1-2y)\right\} \end{aligned} \tag{44}$$

Here $s = \sqrt{2R(1+\lambda)}$.

The results with $\lambda = 0$ corresponding to the Newtonian case are in agreement with those of Rosenblat [1].

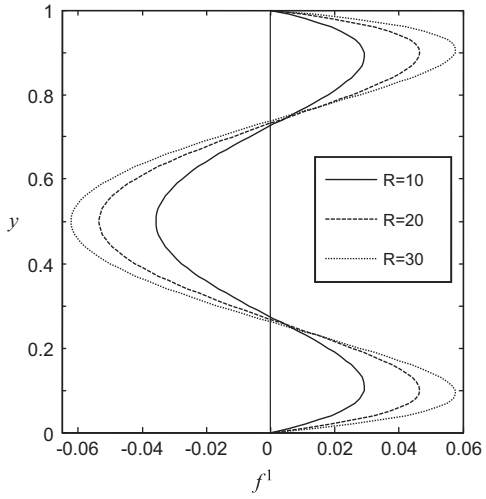

Figure 6 Variation of steady radial velocity f^1 with Reynolds number R for fixed value of $\lambda = 1$.

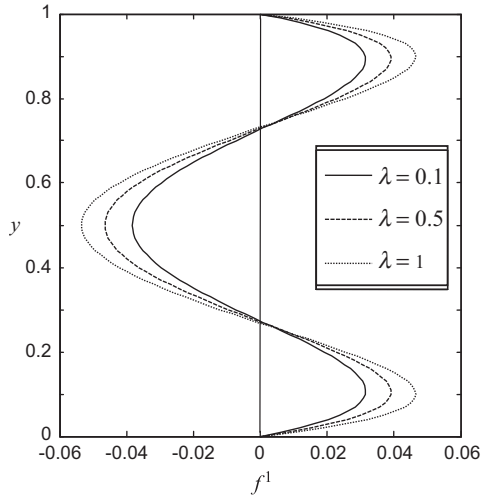

Figure 7 Variation of steady radial velocity f^1 with Jeffrey parameter λ for fixed value of $R = 30$.

3.2.3. Fluctuating radial–axial flow

The solution of (42) for the fluctuating radial–axial flow under the boundary conditions (27) is found to be

$$\frac{\alpha s}{i}\left[\frac{\cosh s\alpha - 1}{\cosh\frac{s\alpha}{2} - 1}\right] h(y)[2 - 2\cosh\beta s + \beta s \sinh\beta s]$$

$$= \left(\alpha s \cosh\frac{s\alpha}{2} - 2\sinh\frac{s\alpha}{2}\right)[\cosh\beta s(1-y) - \cosh\beta s]$$

$$+ \left(\beta s \sinh\beta s \sinh\frac{s\alpha}{2} + \alpha s \cosh\frac{s\alpha}{2} - \alpha s \cosh\frac{s\alpha}{2}\cosh\beta s\right)$$

$$\times (1-2y) - \sinh\frac{s\alpha}{2}(1-2y)[2 - 2\cosh\beta s + \beta s\sinh\beta s] \quad (45)$$

Here $s = \sqrt{2R(1+\lambda)}$ *and* $\alpha = 1 + i$.

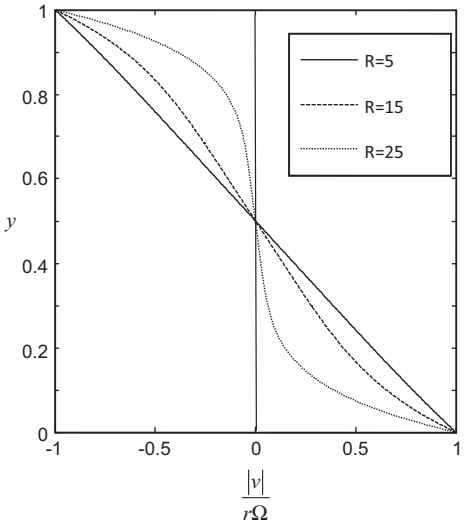

Figure 8 Variation of amplitude of transverse velocity $\frac{|v|}{r\Omega}$ with Reynolds number R for fixed value of $\lambda = 1$.

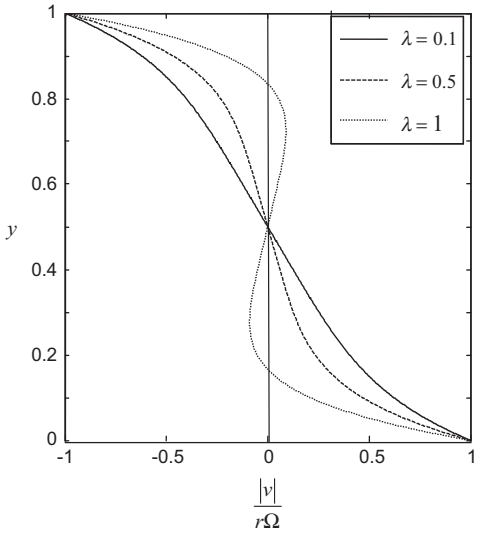

Figure 9 Variation of amplitude of transverse velocity $\frac{|v|}{r\Omega}$ with Jeffrey parameter λ for fixed value of $R = 20$.

4. Results and discussion

In this chapter, the steady laminar flow of incompressible Jeffrey fluid between two torsionally oscillating disks is studied and the transverse velocity, amplitude of transverse velocity and steady radial velocity are numerically computed for certain combination of the parameters and the results are presented graphically in Figs. 2–9. The Figs. 2–5 are drawn for one disk oscillating and the Figs. 6–9 are drawn for two disks oscillating (see Fig. 1).

Fig. 2 is plotted to see the influence of Reynolds number R on the amplitude of transverse velocity $\frac{|v|}{r\Omega}$ for fixed value of $\lambda = 1$. It is observed that, the amplitude of transverse velocity is decreasing with the increase of Reynolds number. When R tends to zero, the velocity profile is linear in y with zero-phase angle.

Fig. 3 is sketched to see the effect of Jeffrey parameter λ on amplitude of transverse velocity $\frac{|v|}{r\Omega}$ for fixed value of $R = 20$. It is observed that, the amplitude of transverse velocity is decreasing with the increase of Jeffrey parameter. When λ tends to zero, the velocity profile is linear in y with zero-phase angle.

Fig. 4 is plotted to find the influence of Reynolds number R on steady radial velocity f' for fixed value of $\lambda = 1$. It is observed that the magnitude of steady radial velocity is increasing with the increase of Reynolds number. The radial velocity is positive in the region $0 \leqslant y \leqslant 0.38$ and is negative in the region $0.38 \leqslant y \leqslant 1$.

Fig. 5 is sketched to find the influence of Jeffrey parameter λ on steady radial velocity f' for fixed value of $R = 20$. It is observed that the magnitude of steady radial velocity is increasing with the increase of Reynolds number. The radial velocity is positive in the region $0 \leqslant y \leqslant 0.38$ and is negative in the region $0.38 \leqslant y \leqslant 1$.

Fig. 6 is plotted to find the influence of Reynolds number R on steady radial velocity f' for fixed value of $\lambda = 1$. It is observed that the magnitude of steady radial velocity is minimum in the middle region and maximum in the regions near the disks and the magnitude of steady radial velocity is increasing with the increase of Reynolds number.

Fig. 7 is sketched to find the effect of Jeffrey parameter λ on steady radial velocity f' for fixed value of $R = 20$. It is observed that the magnitude of steady radial velocity is minimum in the middle region and maximum in the regions near the disks and the magnitude of steady radial velocity is increasing with the increase of Reynolds number.

Fig. 8 is plotted to see the influence of Reynolds number R on amplitude of transverse velocity $\frac{|v|}{r\Omega}$ for fixed value of $\lambda = 1$. It is observed that, the amplitude of transverse velocity is increasing with the increase of Reynolds number. The amplitude is zero at the center of the region.

Fig. 9 is sketched to see the effect of Jeffrey parameter λ on amplitude of transverse velocity $\frac{|v|}{r\Omega}$ for fixed value of $R = 30$. It is observed that, the amplitude of transverse velocity is increasing with the increase of Reynolds number. The amplitude is zero at the centre of the region.

5. Conclusions

1. Due to the oscillations of the lower disk, the radial velocity of the fluid is becoming positive in the lower half of the region ($0 \leqslant y \leqslant 0.5$) and its maximum value increases with the increase in the Reynolds number. The same behavior is observed with variation in Jeffrey parameter λ also.
2. In the case of two disks oscillating, the radial velocity is becoming negative at the central line between the disks and maximum radial velocities occur nearer to the disks. These velocities increase with increasing Jeffrey parameter λ.
3. The amplitude of transverse velocity decreases with increasing Reynolds number or Jeffrey parameter λ in the case of one disk oscillating.
4. When two disks are oscillating, the amplitude of transverse velocity becomes zero in the middle of the region surrounded by oscillating disks.

References

[1] Rosenblat S. Flow between torsionally oscillating disks. J Fluid Mech 1960;8:388–99.
[2] Srivastava AC. Rotating oscillations of an infinite plate in non-Newtonian fluids. Appl Sci Res 1959;9A:369.
[3] Srivastava AC. In: Proc of the symposium on fluid dynamics, Indian Science Congress, (Bombay, India); 1960.
[4] Bhatnagar PL, Rajeswari GK. The secondary flows induced in a non-Newtonion fluid between two parallel infinite oscillating planes. J Indian Inst Sci 1962;44:219–38.
[5] Frater KR. Flow of an elastic viscous fluid between torsionally oscillation discs. J Fluid Mech 1964;19:175.
[6] Verma PD. Flow of visco-elastic Maxwell fluid between torsionally oscillating disks. Proc INSA 1967;39A(4):179.
[7] Verma PD, Chauhan Dileep Singh. Flow between a torsionally oscillating impermeable disk and stationary naturally permeable disk. Indian J Pure Appl Math 1979;10(11):1351–61.
[8] Raghupathi Rao P, Ramachandra Rao A. Flow between torsionally oscillating disks rotating about different axes at different speeds. J Appl Mathemat Phys (ZAMP) 1982;33:358–69.
[9] Dutcher CS, Venerus DC. Compliance effects on the torsional flow of a viscoelastic fluid. J non-Newtonian Fluid Mech 2008;150(2):154–61.
[10] Sharma Pawan kumar, Khan Sabbir. MHD flow in porous medium induced by torsionally oscillating disk. Comput Fluids 2010;39(8):1255–60.
[11] Nadeem S, Akbar NS. Peristaltic flow of a Jeffrey fluid with variable viscosity in an asymmetric channel. Z. Naturforsch 2009;64a:713–22.
[12] Akbar NS, Nadeem S, Ali M. Jeffrey fluid model for blood flow through a tapered artery with a stenosis. J Mech Med Biol 2011;11(3):529.
[13] Nadeem S, Akbar NS, Naz T. The numerical and analytical solution of peristaltic flow of a Jeffrey fluid in an inclined tube with partial slip. J Mech Med Biol 2011;11(4):773.
[14] Akbar NS, Nadeem S. Simulation of variable viscosity and Jeffrey fluid model for blood flow through a tapered artery with a stenosis. Commun Theoret Phys 2012;57:133.
[15] Akbar NS, Nadeem S, Hayat T, Hendi AA. Analytical and Numerical analysis of Vogel's model of viscosity on the Peristaltic flow of Jeffrey fluid. J Aerosp Eng 2012;25(1):64–70.
[16] Akbar NS, Nadeem S, Hayat T, Hendi AA. Effects of heat and chemical reaction on Jeffrey fluid model with stenosis. Appl Anal 2012;91(9):1631–47.
[17] Hayat T, Shehzad SA, Qasim M, Obaidat S. Radiative flow of Jeffrey fluid in a porous medium with power law heat flux and heat source. Nucl Eng Des 2012;243:15–9.
[18] Hayat T, Shehzad SA, Qasim M, Obaidat S. Thermal radiation effects on the mixed convection stagnation-point flow in a Jeffrey fluid. Z. Naturforsch 2011;66a:606–14.
[19] Hayat T, Asad S, Qasim M, Hendi AA. Boundary layer flow of a Jeffrey fluid with convective boundary conditions. Int J Numer Methods Fluids 2012;69:1350–62.
[20] Vajravelu K, Sreenadh S, Lakshminarayana L. The influence of heat transfer on peristaltic transport of a Jeffrey fluid in a vertical porous stratum. Commun Nonlinear Sci Numer Simulat 2011;16:3107–25.

Dr. R. Hemadri Reddy completed Ph.D in the year 2007. His research area is fluid dynamics. He published 2 papers in Springer, four papers in scopus indexed remaining 19 papers are published in peer reviewed journals. He is having 9 years of teaching experience.